Research Article

The Journal of Comparative Neurology
Research in Systems Neuroscience
DOI 10.1002/cne.24449

Sushi repeat-containing protein X-Linked 2 - a novel phylogenetically conserved hypothalamo-pituitary protein

Mehwish Anwer[1], Tamuna Bolkvadze[1], Xavier Ekolle Ndode-Ekane[1], Noora Puhakka[1], Tuomas Rauramaa[2], Ville Leinonen[3], Erwin A van Vliet[4], Dick F Swaab[5], Annakaisa Haapasalo[1], Stina Leskelä[1], Nea Bister[1], Tarja Malm[1], Synnöve Carlson[6], Eleonora Aronica[4], Asla Pitkänen[1*]

[1]*A. I. Virtanen Institute for Molecular Sciences, University of Eastern Finland, Kuopio, Finland.*

[2]*Department of Clinical Pathology, Kuopio University Hospital, Kuopio, Finland.*

[3]*Department of Neurosurgery, Kuopio University Hospital, Kuopio, Finland.*

[4]*Department of (Neuro) Pathology, Academic Medical Center, University of Amsterdam, Amsterdam, the Netherlands.*

[5]*Department of Neuropsychiatric Disorders, Netherlands Institute for Neuroscience, KNAW, Amsterdam, the Netherlands.*

[6]*Department of Neuroscience and Biomedical Engineering, Aalto University, Espoo, Finland.*

***Corresponding author:** Asla Pitkänen, MD, PhD, A. I. Virtanen Institute for Molecular Sciences, University of Eastern Finland, PO Box 1627, FI-70211 Kuopio, Finland, Tel: +358-50-517 2091, Fax: +358-17-16 3030, E-mail: asla.pitkanen@uef.fi

Short Title: SRPX2 in the hypothalamus

Received: Feb 07, 2018; Revised: Apr 03, 2018; Accepted: Apr 04, 2018

Acknowledgments/ Conflict of interest/ Role of authors

Acknowledgments

The study was supported by the Academy of Finland (A.P.), the European Union's Seventh Framework Programme (FP7/2007-2013) under grant agreement N°602102 (EPITARGET; A.P., E.A., E.V.) and the European Union's Horizon 2020 research and innovation programme under the Marie Sklodowska-Curie grant agreement N° 642881 (ECMED; M.A., A.P., E.A.). We thank Mr. Jarmo Hartikainen, Mrs. Merja Lukkari, Dr. Anand M. Iyer, and Mr. Jasper J. Anink for their excellent technical assistance.

Conflict of interest statement

The authors confirm that there are no conflicts of interest.

Author contributions

M.A., X.N., N.P., E.V., and A.P. designed the research

M.A., T.B., N.B., S.L. performed the research

M.A., T.B., X.N., N.P., E.V., A.P. analyzed the data

T.R., V.L., E.A., D.S. provided the human brain tissue, plasma and CSF

S.C. provided the monkey brain tissue

A.H. and T.M. provided the cell lines

M.A. and A.P. wrote the paper with input from all the authors

Abstract

Sushi repeat-containing protein X-linked 2 (SRPX2) is a novel protein associated with language development, synaptic plasticity, tissue remodeling, and angiogenesis. We investigated the expression and spatial localization of SRPX2 in normal mouse, rat, monkey, and human brain using *in situ* hybridization and immunohistochemistry. Antibody specificity was determined using *in vitro* siRNA based silencing of *SRPX2*. Cell type-specific expression was verified by double-labeling with oxytocin or vasopressin. Western blot was used to detect SRPX2 protein in rat and human plasma and cerebrospinal fluid. Unexpectedly, SRPX2 mRNA expression levels were strikingly higher in the hypothalamus as compared to the cortex. All SRPX2 immunoreactive (ir) neurons were localized in the hypothalamic paraventricular, periventricular, and supraoptic nuclei in mouse, rat, monkey, and human brain. SRPX2 colocalized with vasopressin or oxytocin in paraventricular and supraoptic neurons. Hypothalamic SRPX2-ir positive neurons gave origin to dense projections traveling ventrally and caudally towards the hypophysis. Intense axonal varicosities and terminal arborizations were identified in the rat and human neurohypophysis. SRPX2-ir cells were also found in the adenohypophysis. Light SRPX2-ir projections were observed in the dorsal and ventral raphe, locus coeruleus, and the nucleus of the solitary tract in mouse, rat and monkey. SRPX2 protein was also detected in plasma and CSF. Our data revealed intense phylogenetically conserved expression of SRPX2 protein in distinct hypothalamic nuclei and the hypophysis, suggesting its active role in the hypothalamo-pituitary axis. The presence of SRPX2 protein in the plasma and CSF suggests that some of its functions depend on secretion into body fluids.

Key words: Sushi repeat-containing protein X-Linked 2, hypothalamus, paraventricular nucleus, supraoptic nucleus, hypophysis, oxytocin, vasopressin, RRID:AB_2050340, RRID:AB_2157626, RRID:AB_2721268, RRID:AB_90782, RRID:AB_2314534, RRID:AB_321301

Introduction

Sushi repeat-containing protein, X-linked 2 (SRPX2) was first identified as a downstream molecule of the E2A-HLF fusion gene in t(17;19)-positive leukemia cells (Kurosawa et al., 1999). Later, SRPX2 expression was reported in neuronal cells located in speech and vocalization-related areas, and two mutations (Y722S or N327S) of the *SRPX2* gene were identified in patients with Rolandic epilepsy associated with speech dyspraxia, mental retardation, and bilateral perisylvian polymicrogyria (Roll et al., 2006). The contribution of the mutated *SRPX2* gene to epilepsy has been questioned because the patients also carried a mutation in *GRIN2A* gene (Lesca et al., 2013). *SRPX2* mutations are, however, considered to cause language impairment which is supported by studies showing that SRPX2 is highly expressed in the language cortex and *SRPX2* silencing impairs ultrasonic vocalizations in mice (Roll et al., 2006; Sia, Clem, & Huganir, 2013). SRPX2 interacts with the urokinase-type plasminogen activator receptor (uPAR) and the SRPX2-uPAR interaction initiates neuronal migration in the cerebral cortex and increases spine density in distal dendrites, resulting in increased cortical excitability (Salmi et al., 2013). The SRPX2-uPAR interaction is regulated by the transcription factor FOXP2, mutations of which cause severe speech and language disorders (MacDermot et al., 2005; Royer-Zemmour et al., 2008).

Studies of glioblastoma (Tang et al., 2016a), gastric cancer (Tanaka et al., 2009), liver cancer (Lin, Chang, Wang, Tian, & Yu, 2017), and colorectal cancer (K. L. Liu, Wu, Zhou, & Fan, 2015; Øster et al., 2013) showed that SRPX2 is a secreted protein whose expression increases angiogenesis and adhesion of cancer cells. An increased level of tissue SRPX2 is a predictive biomarker for a poor outcome in patients with hepatocellular carcinoma (Lin et al., 2017). The function of SRPX2 in cancer cells requires interaction with uPAR on the cell surface and engagement of membrane co-receptors, such as $\alpha_v\beta3$ integrin and PDGFRβ receptors. This results in intracellular activation of the P12k/Akt, Ras/MAPK, and P-FAK/Akt pathways, eventually activating MMP2 and MMP9 matrix metalloproteinases (Lin, Chang, Wang, Tian, & Yu, 2017; K. Liu, Fan, & Wu, 2017; Tang et al., 2016b; Yamada et al., 2014). Expression of *SRPX2* in colorectal cancer is regulated by non-CpG island promoter hypomethylation and post-transcriptionally by miR-149 (Øster et al., 2013).

The well-defined effects of SRPX2 on language learning, angiogenesis, and synaptic plasticity make SRPX2 a promising target to modulate tissue repair after brain injury or disease. Surprisingly, there are no descriptions of the cellular localization of SRPX2 in the cortical and subcortical areas

of the brain, and of possible species differences. Therefore, we investigated the spatial distribution of SRPX2 protein in normal mouse, rat, monkey and human brain, and profiled the neurons expressing SRPX2 protein. As we observed SRPX2 in hypothalamo-pituitary projections, we also determined its presence in the plasma and cerebrospinal fluid (CSF).

Materials and Methods

Specificity of SRPX2 antibody

Cell line selection. We first confirmed the specificity of rabbit anti-SRPX2 antibody (ab91584, Abcam), which was used in most of the immunostainings, by *in vitro* siRNA based silencing of SRPX2 protein in cell cultures. In order to select a suitable cell line, we screened one primary and six secondary cell cultures for endogenous expression of SRPX2 using RT-qPCR and Western blot. Among these, mouse P19 embryonal carcinoma derived cells, mouse N2a neuroblastoma cell line, human n2012 teratocarcinomas cells, primary mouse E18 cortical cells, differentiated iPSCs cells, and human SH-SY5Y neuroblastoma cells all endogenously expressed *SRPX2* mRNA. SH-SY5Y cells with abundant expression of *SRPX2* mRNA and protein were selected for transfection with *SRPX2* siRNA and subsequent antibody validation.

SH-SY5Y were cultured and maintained in DMEM/F12 + GlutaMAX (Dulbecco's Modified Eagle Medium/Nutrient Mixture F-12, Gibco, Gaithersburg, MD, USA) with PenStrep (penicillin-streptomycin, 100 units/ml) as antibiotics. All cells were maintained at 37°C in a 5% CO_2 atmosphere. Cells were plated into 12-well plates (150,000 cells/well) for siRNA transfection and allowed to adhere overnight.

siRNA transfection. Pre-designed *Silencer®* siRNA against human *SRPX2* mRNA was used (AM16708, Ambion) for transfection of SH-SY5Y cells using Lipofectamine® 2000 (Thermo Fisher Scientific). *Silencer®* FAM-labeled negative control siRNA (AM4620, Ambion) was transfected parallel to *SRPX2* siRNA to ensure transfection efficiency and specificity. Transfection was carried out according to manufacturer's protocol. Briefly, cells were treated with *SRPX2* siRNA (10-50 nM) or negative control siRNA (10-50 nM) for 48 h. Untreated cells were processed at the same time for comparison and all the transfections were carried out in triplicate. After 48 h, the cells were

washed with PBS and frozen at -70^{o}C overnight. Transfection outcome was evaluated using a systematic approach. First, RNA from mock-transfected and *SRPX2* siRNA transfected cells was assayed for *SRPX2* mRNA quantification by RT-qPCR, and the transfection conditions were optimized until a more than two-fold reduction in the transcript was achieved. Then, the optimized transfection was evaluated for antibody specificity using Western blotting and immunofluorescence staining.

***Real-time quantitative PCR*.** RT-qPCR analysis was carried out to test the reduction in *SRPX2* mRNA after transfection. Total RNA was harvested using AllPrep DNA/RNA Mini Kit (QIAGEN®, Hilden, Germany), quantified by NanoDrop™ (ND-1000) and evaluated for quality by checking the RNA Integrity Number (RIN) (Agilent Bioanalyzer). Samples with RIN 9 and above were included in the analysis. cDNA from 0.5 µg of total RNA was synthesized using high-capacity RNA-to-cDNA Kit (Applied Biosystems, Foster City, CA, USA) and amplified using TaqMan® Gene Expression Master mix (Applied Biosystems). The human SRPX2 TaqMan® gene expression assay (Hs00997580, Thermo Fisher Scientific) was used for *SRPX2* mRNA amplification. As a stable endogenous control, β-actin was measured simultaneously (Armstrong et al., 2007) using the human ACTB TaqMan® assay (Hs03023943-g1, Thermo Fisher Scientific). The program for RT-qPCR reaction was as follows: one cycle (50^{o}C-120 sec), one cycle (95^{o}C-600 s) and 50 cycles (95^{o}C -15 s, 60^{o}C-60 s). All assays were performed according to the manufacturer's protocol. *SRPX2* mRNA level values were normalized to *ACTB* mRNA levels and expressed as fold-increase relative to gene expression in untreated control cells. The relative expression level (fold change) of the target gene was calculated using the $2^{-\Delta\Delta CT}$ method and the knockdown percentage (%KD) was calculated using the equation, $\%KD = (1-\Delta\Delta C_T)*100$, where, $\Delta\Delta C_T$ is the normalized expression of the target (Schmittgen & Livak, 2008). Data were analyzed using IBM SPSS 19.0 for Windows (SPSS Inc., Chicago, IL, USA).

MTT Cell Viability Assay. SH-SY5Y cells were seeded into 48-well plates (37,500 cells/well), transfected for 48 h and incubated with colorimetric 3-(4,5-dimethylthiazol-2)-2,5-diphenyltetrazolium bromide (MTT, M2128, MilliporeSigma) for 3 h at 37^{o}C. Formazan precipitates were dissolved in 200 µl DMSO at RT for 4h. The solution was measured for its optical density (OD) at the 595 nm. Data are expressed as a percentage of the mean absorbance of untreated cells.

Western blot. After confirming transfection with RT-qPCR, the transfection was repeated and cells were used to evaluate the specificity of rabbit polyclonal antibody raised against human SRPX2 (ab91584, Abcam) by Western blotting. The transfected frozen SH-SY5Y cells were lysed by

directly adding 1x RIPA lysis buffer containing protease inhibitor cocktail to the wells for 30 min. The lysate was centrifuged at 2,800g for 15 min at 4^{o}C to pellet the cell debris and the supernatant was stored at -70^{o}C until use. Total protein concentration was measured using a Pierce BCA Protein Assay Kit (Thermo Fisher Scientific) to load equal amounts of protein in each well. Therefore, a mixture of lysate (20 µg of protein), 1X Laemmli buffer, and β-Mercaptoethanol were heated at 90^{o}C, separated by SDS-polyacrylamide gel electrophoresis (SDS-PAGE) and transferred to nitrocellulose membranes. The membranes were blocked for 2 h in 1X TEN-1% Tween20 solution and incubated overnight at 4°C with rabbit polyclonal anti-SRPX2 (1:1000, ab91584, Abcam) or mouse monoclonal anti-β-actin (1:1000, sc-47778, Santa Cruz Biotechnology, Dallas, TX, USA) antibody. The blots were then incubated with HRP goat anti-rabbit (1:2000, 65-6120, Invitrogen) and goat anti-mouse (1:2000, 62-6520, Invitrogen) secondary antibodies for 1h at RT. Immunoreactive bands were visualized using enhanced chemiluminescence substrate (SuperSignal™ West Pico Chemiluminescent Substrate, Thermo Fisher Scientific) on a gel documentation system (GelDoc Bio-Rad).

Immunofluorescence (IF) staining of fixed siRNA transfected cells. SH-SY5Y cells were grown on coverslips in 12 well plates. The cells were rinsed with PBS, fixed in 4% PFA solution for 15 min (at RT), rinsed with 1× PBS, permeabilized with 0.1% Triton-X100 for 2 min, and then incubated with the rabbit anti-SRPX2 antibody (1:1000, ab91584, Abcam) for 1 h followed by anti-rabbit Alexa488 (1:200, ab150117, Abcam) or anti-rabbit Alexa568 secondary antibody (1:200, ab175695, Abcam) for 1 h at RT. The coverslips were mounted on glass slides and sealed with VectaShield containing DAPI (H-1200, Vector).

Processing of tissue for histology

Mouse and Rat. Adult (14 weeks of age, 290–350 g) male Sprague-Dawley rats (Envigo Laboratories S.r.l., Udine, Italy) and adult (12 weeks, 20–30 g) male C57BL/ 6J mice (The Jackson Laboratory, Bar Harbor, ME, USA) were used to obtain brain tissue and plasma (rats only) samples. The animals were housed in a controlled environment (temperature 22 ± 1^{o}C, humidity 50%–60%, light–dark cycle from 07.00 to 19.00 h) with free access to food and water. All animal procedures were approved by the Animal Ethics Committee of the Provincial Government of Southern Finland, and performed in accordance with the guidelines of the European Community Council Directives

2010/63/EU. The rodents used in the study are not maintained under SPF conditions. However, the animals are maintained according to FELASA recommendations for health monitoring of rodents and quarterly screened for harmful agents.

For immunohistochemistry, the mice were deeply anesthetized with a mixture of 18.75 mg/mL ketamine and 0.25 mg/mL medetomidine (4 mL/kg, i.p.) and rats with a cocktail of sodium pentobarbital (58 mg/kg), magnesium sulfate (127.2 mg/kg), propylene glycol (42.8%), and absolute ethanol (11.6%) (6 mL/kg, i.p.). The animals were transcardially perfused with 0.9% saline (mice: 5 ml/min, rats: 30 ml/min at 4^{o}C) for 3 min followed by 4^{o}C paraformaldehyde (PFA) in 0.1 M sodium phosphate buffer, pH 7.4 (mice: 5 ml/min, rats: 30 ml/min at 4^{o}C), for 15 min. The brain (and hypophysis where possible) was removed from the skull and post-fixed in 4% PFA for 4 h (at 4^{o}C), and then cryoprotected in a solution containing 20% glycerol in 0.02 M potassium phosphate buffered saline (KPBS) for 24 h. The brains were then frozen on dry ice and stored at -70^{o}C until cut. The mouse and rat brains were sectioned in a coronal plane (25 µm and 30 µm, respectively) in 1-in-5 series with a sliding microtome (Leica SM 2000, Leica Microsystems Nussloch GmbH, Nussloch, Germany). The first series of sections was collected in 10% formalin at room temperature (RT) for thionin staining. The remaining series of sections were stored in tissue collecting solution (TCS: 30% ethylene glycol, 25% glycerol in 0.05 M sodium phosphate buffer) at -20^{o}C until staining.

For *in situ* hybridization, rat brains were fixed in 10% buffered formalin and embedded in paraffin. Sagittal sections (6 µm) were cut using a microtome, collected on glass slides, and stored at room temperature (RT) until use.

***Monkey*.** Hypothalamic and brainstem sections from two female adult *Macaca arctoides* monkeys (weight 7-8 kg) were used for SRPX2 immunohistochemistry. The maintenance of the monkeys and all procedures of the study were carried out according to the Finnish law and statutes governing animal experimentation. The Finnish Ministry of Agriculture had approved of the studies performed on monkeys.

The monkeys were deeply anesthetized with a cocktail of Ketalar (1ml) and Nembutal (4.5ml). The animals were perfused intracardially with 0.9% saline (250ml/min) for 2 min at RT followed by a solution of 4% PFA and 0.1% glutaraldehyde in 0.1 M sodium phosphate buffer for 10 min at the rate of 250ml/min and then 50 min at the rate of 100ml/min. The brain was removed from the skull and post-fixed for 2 h at 4^{o}C in the above fixative. The brain tissue was then cryoprotected in

10% glycerol and 2% dimethylsulfoxide (DMSO) solution for 24 h, in 20% glycerol and 2% DMSO solution for 3 days at 4°C, and then frozen by immersion in ice cold isopentane (2-methyl butane). Coronal sections of the brain (30 µm) were cut in a 1-in-8 series and stored in TCS at -70°C until stained.

Human. Autopsy (24 hours post-mortem) human brain tissue (hypothalamus and hypophysis, n=5), from adult subjects without a diagnosed brain pathology (Male, 48-85 years old, cause of death: myocardial infarction) were obtained from Kuopio University Hospital, Kuopio, Finland, and Academic Medical Center, University of Amsterdam, The Netherlands and the Netherlands Brain Bank. Tissues were obtained and used in accordance with the Declaration of Helsinki and Institutional Review Board approvals. Consent for autopsy was obtained in concordance with institutional regulations.

For immunohistochemistry, the hypothalamus and hypophysis were fixed in 10% formalin solution for 48 h, followed by cryoprotection for 48 h in a solution containing 20% glycerol and 2% DMSO in 0.1 M sodium phosphate buffer. The tissue was then immersed in ice-cold isopentane, and frozen blocks were stored at -70°C until cut. The blocks containing hypothalamus and hypophysis were cut into 30-µm-thick coronal sections (1-in-8 series) using a sliding microtome. Free-floating sections were stored at -70°C in tissue collecting solution (TCS: 30% ethylene glycol, 25% glycerol in 0.05 M sodium phosphate buffer) until used for immunohistochemistry.

For *in situ* hybridization, 6-µm-thick coronal sections were cut from paraffin embedded human tissue and collected on glass slides. The slides were dried and stored at RT until use.

Nissl staining

To identify the cytoarchitectonic boundaries of different brain areas to optimize the selection of sections for analyses, the first series of sections was used for Nissl staining (Huusko, Römer, Ndode-Ekane, Lukasiuk, & Pitkänen, 2015). The sections were mounted on glass slides coated with 0.5% gelatin (G-2500, MilliporeSigma, Burlington, MA, USA), rehydrated in decreasing grades of alcohol, stained for thionin, dehydrated in increasing grades of alcohol and cover-slipped with mounting medium (Depex® BDH Chemical, Poole, UK).

In situ hybridization

In situ hybridization for *SRPX2* mRNA was performed on rat and human hypothalamic sections using 5'–3' double digoxygenin (DIG)-labeled probe, containing locked nucleic acid [LNA] and 2'O-methyl [2'OMe] RNA moieties (Exiqon, Vedbaek, Denmark). To detect both rat (NM_001108243.2) and human (NM_014467.2) *SRPX2* mRNA, the probe was designed using a conserved sequence 5'DIG-LTmCmULGmCmALTmAmULAmCmULTmCmALTmUmGLT-DIG-3', where "L" indicates LNA and "m" indicates [2'OMe] RNA moieties (Exiqon). Briefly, the sections were deparaffinized in xylene and graded ethanol (100% and 70%) for 3 min each. Endogenous peroxidase activity was blocked by incubating the sections in 0.3% H_2O_2 in methanol for 20 min. After washing with sterile water, the sections were immersed in Na-citrate buffer (pH 6), and heated at 95^{o}C for 10 min to improve tissue permeability. The sections were then hybridized with the *SRPX2* mRNA probe (250 nM) in the hybridization mix (50% deionized formamide, 600 mM NaCl, 10 mM HEPES buffer, pH 7.5, 1 mM EDTA, 5X Denhardt's reagent) at 56°C for 1 h. After hybridization, the tissue sections were washed with 2X SSC (saline sodium citrate, pH 5), 0.5X SSC and 0.2X SSC buffers for 2 min each at 56^{o}C. The sections were blocked for 15 min with phosphate buffered saline (PBS) containing 1% bovine serum albumin, 0.02% Tween 20, and 1:100 normal goat serum (NGS). Sheep anti-DIG alkaline phosphatase (AP) (1:1500, 1093274, Roche) prepared in blocking buffer was added to the sections for 1 h at RT. NBT (nitro-blue tetrazolium chloride)/BCIP (5-bromo-4-chloro-30-indolyphosphate p-toluidine salt) was used as chromogenic substrate for AP to detect the SRPX2 mRNA hybridization. The slides were mounted with VectaMount at RT.

For double-labeling, *in situ* hybridization was followed-up by immunohistochemistry. Briefly, after developing the chromogenic reaction for SRPX2 mRNA, the slides were washed with PBS, blocked with PBS containing NGS, and incubated with anti-SRPX2 antibody for 1 h at RT, followed by three washes with PBS, and then incubated with horseradish peroxidase (HRP)-labeled anti-rabbit secondary antibody (BrightVision+ kit, DPVB110HRP, Immunologic, Duiven, the Netherlands) for 1 h at RT. The antigen was visualized by chromogen 3-amino-9-ethylcarbazole (AEC, A-5754, MilliporeSigma) solution containing 0.1% H_2O_2 in 0.05 M acetate buffer for 8 min. Negative control assays performed without probes and without the primary antibody were blank.

Immunohistochemistry

Mouse and Rat. A 1-in-5 series of coronal sections was stained for SRPX2 protein following the protocol described earlier (Ndode-Ekane, Hayward, Gröhn, & Pitkänen, 2010). Briefly, sections were washed in 0.02 M KPBS (pH 7.4) incubated with 1% H_2O_2 to reduce the endogenous peroxidase activity, blocked in 10% NGS and 0.5% Triton X-100. The sections were incubated in rabbit polyclonal antibody raised against SRPX2 (1:10,000, ab91584, Abcam, Cambridge, UK, RRID:AB_2050340), 1% NGS, and 0.5% Triton X-100 in KPBS at 4^{o}C for 2 nights. After washing with KPBS, the sections were then incubated for 1 h in biotinylated goat anti-rabbit IgG antibody (1:200, BA-1000, Vector Laboratories, Burlingame, CA, USA) followed by 1% avidin-biotin enzyme complex ABC (Vectastatin® ABC kit, PK4000, Vector Laboratories) solution for 45 min. The antigen was visualized using 0.1 % 3,3'- diaminobenzidine (Pierce Chemical, Rockford, IL, USA) solution containing 0.4% H_2O_2 in KPBS for 1 min. The sections were picked up on the glass slides and dried overnight at37°C. The staining reaction was intensified using 0.005% osmium tetroxide (OsO4, #19170, Electron Microscopy Sciences, Hatfield, PA, USA) as previously described (Lewis, Campbell, & Morrison, 1986). Slides were covered with Depex ® and dried overnight in the hood.

Monkey and Human. The protocol for immunohistochemistry was the same as used for rodent tissue, except that the sections were pre-treated with 1% sodiumborohydride for 15 min before blocking. In human, sections containing hypothalamus were stained. In monkeys, sections including the brainstem were also stained.

Estimation of the number of SRPX2 positive neurons in rat and mouse hypothalamus using unbiased stereology. SRPX2 immunopositive cells throughout the rostrocaudal axis of hypothalamus (using sections from a 1-in-10 series) were plotted using the AccuStage MDPlot 5.3 software and MD3 Microscope Digitizer (AccuStage, Shoreview, MN, USA) connected to a Leica DMRB microscope. The cytoarchitectonic boundaries of Pa, Pe, and SO nuclei were then drawn on computer-generated plots from the adjacent thionin-stained sections with the aid of a *camera lucida* stereomicroscope equipped with a drawing tube. The total number of cells (N_{tot}) was calculated per region (Pa, Pe, and SO) according to the following formula: $N_{tot} = \sum Q \times 1/ssf$, where $\sum Q$ is the sum of cells counted from all sections and ssf is the section sampling fraction (1/10) (West, Slomianka, & Gundersen, 1991). Data is expressed as mean ± SEM.

Immunofluorescence double-labeling. To identify the cell types expressing SRPX2, rat hypothalamic sections were double-labeled with either oxytocin or vasopressin antibodies.

For double-labeling with oxytocin, the sections were washed with KPBS, incubated with 1% NGS in KPBS containing 0.5% Triton X-100, and then, incubated overnight with rabbit polyclonal anti-SRPX2 antibody (1:1000, ab91584, Abcam). After washing with PBS, the sections were incubated with anti-rabbit Alexa488 antibody (1:200, ab150077, Abcam) for 2 h, washed again with PBS, and incubated overnight with mouse anti-oxytocin antibody (1:5000, MAB5296, MilliporeSigma, RRID:AB_2157626). The sections were washed in PBS and then incubated with anti-mouse Alexa 647 antibody (1:200, ab150115, Abcam) for 2 h. Sections were mounted on slides, cover-slipped with VectaMount and sealed with nail enamel.

For double-labeling with vasopressin, the sections were washed with KPBS, immersed in Na-citrate buffer (pH 6), and heated at 95^{o}C for 10 min. After rinsing with tap water, the sections were incubated with 1% NGS in KPBS containing 0.5% Triton X-100, and then, incubated overnight with mouse monoclonal anti-SRPX2 antibody (1:1000, 66266-1, Proteintech, Rosemont, IL, USA RRID:AB_2721268). After washing with PBS, the sections were incubated with anti-mouse Alexa 488 antibody (1:200, ab150117, Abcam) for 2 h, washed again with PBS and incubated overnight with rabbit anti-vasopressin antibody (1:5000, AB1565, Chemicon, Darmstadt, Germany, RRID:AB_90782). The sections were washed in PBS and then incubated with anti-rabbit Alexa 568 antibody (1:200, ab175695, Abcam) for 2 h. Sections were mounted and cover-slipped with VectaMount and sealed with nail enamel.

To estimate the percentage of SRPX2 positive cells that also express oxytocin, 10 photomicrographs were captured from 3 rat brains (2 sections from each animal) using 40x magnification, resulting in 5-10 cells per photomicrograph for colocalization estimation. The number of immunolabeled cells for each antibody were counted in the Pa and SO nuclei of the hypothalamus.

For double-labeling with astrocyte marker, GFAP, and microglia marker, OX-42, the sections were washed with KPBS, incubated with 1% NGS in KPBS containing 0.5% Triton X-100, and then, incubated overnight with either mouse monoclonal anti-GFAP antibody (1:2000, Cat# 814369, Boehinger Mannheim, RRID:AB_2314534) or mouse monoclonal OX-42 (1:2000, MCA275G, Bio-Rad/AbD Serotec, RRID:AB_321301). After washing with PBS, the sections were incubated with anti-mouse Alexa 488 antibody (1:200, ab150117, Abcam) for 2 h, washed again with PBS, and incubated overnight with rabbit anti-SRPX2 antibody (1:5000, ab91584, Abcam). The sections were washed in PBS and then incubated with anti-rabbit Alexa 568 antibody (1:200, ab175695, Abcam)

for 2 h. Sections were mounted on slides, cover-slipped with VectaMount and sealed with nail enamel.

SRPX2 western blot from rat and human plasma and human CSF

Rat Plasma. Blood samples were obtained from the lateral tail vein of adult male rats (n=10) under isoflurane anesthesia. The samples were centrifuged (1,300g for 10 min at 4^{o}C), plasma was aliquoted and stored at -70^{o}C (van Vliet et al., 2017).

Human plasma. Blood samples were obtained from the cubital vein of healthy adult male and female subjects (n=3) at Kuopio University Hospital between 7 am – 8 am. The samples were centrifuged (2,200g for 10 min at RT), plasma was collected and stored at -70°C.

Human CSF. CSF samples (n=3) were obtained through lumbar puncture performed at Kuopio University Hospital between 9 am – 11 am. After brief mixing, the samples were centrifuged (2,000g for 10 min at RT), supernatant was collected and stored at -70^{o}C.

Western blot. Total protein concentration in plasma and CSF was measured using Pierce BCA Protein Assay Kit (23225, Thermo Fisher Scientific). Plasma samples were diluted with PBS to adjust the protein concentration to 2 µg/µl for Western blot analysis. The diluted plasma (20 µg protein, final volume 25 µl) or 60 µl undiluted CSF, 1X Laemmli buffer, and β-Mercaptoethanol were heated at 90^{o}C, separated on 12% TGX Stain-Free™ gels (Bio-Rad, Hercules, CA, USA) by SDS-polyacrylamide gel electrophoresis (SDS-PAGE) and transferred to nitrocellulose membranes. The membranes were blocked for 2 h in 1X TEN-1% Tween20 solution and incubated overnight at 4^{o}C with rabbit polyclonal anti-SRPX2 (1:1000, ab91584, Abcam). The blots were then incubated with HRP goat anti-rabbit (1:10000, 65-6120, Invitrogen, Carlsbad, CA, USA) antibody for 1 h at RT. Immunoreactive bands were visualized using enhanced chemiluminescence substrate (SuperSignal™ West Pico Chemiluminescent Substrate, Thermo Fisher Scientific) on a gel documentation system (GelDoc Bio-Rad).

Results

Specificity of SRPX2 antibody

As there are no prior reports on the immunohistochemical location of SRPX2 in hypothalamic neurons, we first confirmed the specificity of the antibody using small interfering RNA (siRNA) to silence the *SRPX2* mRNA *in vitro*. We screened cell lines for endogenous SRPX2 expression and selected the human SH-SY5Y neuroblastoma cells for siRNA transfection **(Fig 1, a-c)**. After transfection, we analyzed *SRPX2* mRNA expression using RT-qPCR **(Fig 1, d)** and SRPX2 protein expression using Western blot **(Fig 1, e)** and immunofluorescence **(Fig 1, f-h)**.

RT-qPCR analysis showed a dose-dependent reduction in the *SRPX2* mRNA following transfection of SH-SY5Y cells with 10-50 nM siRNA. The knockdown percentage (%KD) of *SRPX2* mRNA was 54% (46% remaining, untreated vs. 30 nM transfection) using 30 nM and 87% (13% remaining, untreated vs. 50 nM transfection) using 50 nM *SRPX2* siRNA as compared with untreated cells after normalization with internal control *ACTB* **(Fig 1, d)**. The mock transfection at same concentrations did not result in *SRPX2* mRNA reduction.

The protein level of SRPX2 in the Western blot was dose-dependently reduced when the cells were transfected with the aforementioned siRNA concentrations. The reduction in the intensity of the 53 kDa immunolabeled band emphasized the specific reduction of the SRPX2 protein levels **(Fig 1, e)**. Immunofluorescence staining of SH-SY5Y cells transfected with 50 nM siRNA, using the same anti-SRPX2 antibody, confirmed a marked reduction in SRPX2 protein as compared with untreated and mock-transfected cells **(Fig 1, f-h).**

The transfection efficiency was evaluated under a microscope by FAM-labeled negative control siRNA, which was localized inside the cell after 24 h of transfection **(Fig 1, i)**. The cell viability assay showed an approximately 17% decrease in cell numbers of the transfected wells when compared to untreated cells and normalized with the absorbance of the dead cell control and media only. This change was comparable in all transfections and not due to anti-SRPX2 siRNA transfection **(Fig 1, j).** All of the above findings confirmed the specificity of the SRPX2 antibody used in this study.

SRPX2 expression in normal brain

In order to identify the precise location of SRPX2 mRNA in normal brain, we labeled sections from rat **(Fig 2, a)** and human brain **(Fig 2, b)** using *in situ* hybridization. High levels of SRPX2 expression were detected in the hypothalamic paraventricular (Pa), periventricular (Pe) and supraoptic (SO) nuclei. We then stained brain sections for SRPX2 protein using immunohistochemistry **(Fig 2, c-d)** with a SRPX2 antibody (polyclonal rabbit anti-SRPX2, ab91584, Abcam). The staining showed immunoreactivity in the same regions of the rat **(Fig 2, c)** and human **(Fig 2, d)** hypothalamus. SRPX2 expression was only detected in neurons **(Fig 2, h-m)** and was mainly cytoplasmic. Combining *in situ* hybridization and immunohistochemistry confirmed the colocalization of SRPX2 mRNA and SRPX2 protein **(Fig 2, e)**. Immunolabeling in the hypothalamic sections was performed using two different antibodies and the staining pattern was reproduced with the second antibody against SRPX2 protein (mouse monoclonal anti-SRPX2 antibody, 66266-1, Proteintech) **(Fig 2, f)**. RT-qPCR and *in situ* hybridization revealed a relatively weak SRPX2 mRNA expression in human cortex as compared with the hypothalamus **(Fig 2, g).**

SRPX2 is expressed in hypothalamic neurons and its distribution is highly conserved between rodents and primates

Rat. In rat brain, all SRPX2-ir neurons were located in the hypothalamus **(Fig 3, a)**, particularly in the Pa, Pe **(Fig 3, a_1)**, and SO nuclei **(Fig 3, a_2)**. In the Pa, SRPX2-ir neurons were distributed bilaterally in all functional compartments within the nucleus, including the neurosecretory magnocellular neurons, endocrine, and pre-autonomic parvocellular neurons (Ferguson, Latchford, & Samson, 2008; Loewen et al., 2017; Swanson & Sawchenko, 1983). The cytoplasmic SRPX2 protein had a granular appearance when observed at a higher magnification **(Fig 3, c)**. In the Pe, SRPX2-ir cells were scattered along its complete rostro-caudal axis. The SO nucleus exhibited strong SRPX2 immunoreactivity. A few scattered SRPX2-ir neurons were also observed in the supraoptic decussation part and the nucleus circularis. Stereological cell counting revealed 2495 ± 215 SRPX2 neurons in the Pa (32% of all SRPX2-ir neurons in the hypothalamus), 835 ± 94 in the Pe (11% of all ir neurons), and 4520 ± 292 in the SO nucleus (58% of all ir neurons).

Hypothalamic SRPX2-ir neurons gave origin to a dense projection that traveled ventrally and caudally towards the hypophysis **(Fig 3, b)**. SRPX2-ir passing fibers were almost exclusively localized in the internal layer of the median eminence, which matches with the presence of SRPX2 immunoreactivity in the neurons of the Pa and So nuclei of the hypothalamus **(Fig 4, a-b)**. Sparse projections to the dorsal and ventral raphe, locus coeruleus, and nucleus of the solitary tract were also observed **(Fig 4, b-c)**. Few immunolabeled fibers traveled through the pontine reticular nucleus and the intermediate reticular nucleus. Very few SRPX2-ir fibers were observed in the lateral septal nucleus and the anteroventral periventricular nucleus. A very light short varicose SRPX2 projection was found in the dorsal part of the central division of the medial nucleus and in the anterior cortical nucleus of the amygdaloid complex. No axonal staining was found in the cerebral cortex.

Mouse. Like in rat, also in the mouse brain SRPX2-positive neurons were exclusively located in the hypothalamus **(Fig 3, d)**. In the mouse hypothalamus, the estimated total number of SRPX2-ir neurons was 1843 ± 303 in the Pa (58% of all ir neurons), 503 ± 85 in the Pe (16% of all SRPX2-ir neurons in the hypothalamus), and 837 ± 108 in the SO nuclei (26% of all ir neurons). Also like in rat, we detected no immunoreactivity in the cortex.

Monkey and human. Analysis of monkey and human hypothalamic sections indicated that the spatial distribution of hypothalamic SRPX2-ir neurons was consistent among rodents and primates **(Fig 3, e-f).**

SRPX2 colocalizes with oxytocin or vasopressin in the hypothalamus

The Pa and SO nuclei synthesize oxytocin and vasopressin, which are then transported to the hypophysis, and secreted into the blood stream (Swanson & Sawchenko, 1983). As the light-microscopic location of SRPX2 in the Pa and SO suggested colocalization, we next performed double-labeling of SRPX2 with oxytocin or vasopressin in the rat hypothalamus. Approximately 88% of SRPX2-ir neurons in the Pa and 61% in the SO were also immunoreactive for oxytocin **(Fig 5, a-c)**. Double-immunofluorescence also indicated colocalization of SRPX2 with vasopressin **(Fig 5, d-f)**.

SRPX2 in the hypophysis

We observed heavy axonal projections from the rat hypothalamic SRPX2-ir neurons to the hypophysis. In the rat posterior pituitary, we found dense terminal arborizations **(Fig 5, g-h)**. In the human neurohypophysis, SRPX2 immunoreactivity was observed in the terminals and axonal Herring bodies **(Fig 5, j-k)**. The cells in the rat **(Fig 5, i)** and human **(Fig 5, l)** adenohypophysis exhibited cytoplasmic vesicle-like SRPX2 immunoreactivity.

SRPX2 protein in plasma

After determining the distribution of SRPX2 in the brain, we investigated whether SRPX2 protein is secreted to rat and human blood, and CSF. Using Western blot, we detected a 53 kDa SRPX2 immunoreactive band in rat and human plasma with two different SRPX2 antibodies. SRPX2 protein was also detected in human CSF from the same cases **(Fig 5, m)**. SRPX2 protein was detected in both male and female human plasma and CSF samples.

Discussion

We report a phylogenetically conserved neuronal expression of SRPX2 protein in the Pa, Pe, and SO nuclei of the mouse, rat, monkey, and human hypothalamus, and SRPX2-ir projections to the neurohypophysis and brainstem **(Fig 6)**. We also demonstrated the colocalization of SRPX2 protein with oxytocin or vasopressin, and show SRPX2 protein in rat and human plasma, and human CSF. In addition, we validate the specificity of anti-SRPX2 antibody according to the recommendations of International Working Group for Antibody Validation (Uhlen et al., 2016).

SRPX2 has been identified as a language-associated protein and *in utero* silencing of SRPX2 impairs ultrasonic vocalizations in mouse pups (Sia et al., 2013). This is consistent with human studies suggesting an association of *SRPX2* and *FOXP2* gene mutations with language impairment (Roll et al., 2006, 2010; Sia et al., 2013). Surprisingly, we found that SRPX2 protein was expressed in the hypothalamic nuclei instead of the ultrasonic vocalization related temporal cortex in mice and rats. We employed multiple staining strategies to verify the staining pattern. Fresh frozen, fixed frozen and paraffin embedded tissue was used for immunohistochemistry using two

different antibodies. We also used 10 mM sodium citrate buffer (pH 6 at 95°C) in rat tissue, and sodium borohydride in monkey and human brain tissue. However, none of these approaches showed distinct SRPX2 immunoreactivity in the cortex. Hypothalamic staining was consistently detected in all types of staining strategies.

The SRPX2 protein colocalized with oxytocin or vasopressin in the Pa and SO nuclei. This suggests a role of SRPX2 in neuroendocrine functions. Interestingly, oxytocin-expressing neurons in the Pa have an important role in social communication, including vocal learning and language (Pfundmair, Lamprecht, von Wedemeyer, & Frey, 2016; Theofanopoulou, Boeckx, & Jarvis, 2017; Ye, Stolk, Toni, & Hagoort, 2016; Zhang et al., 2016). Similar to SRPX2, oxytocin knockout mice exhibit reduced ultrasonic vocalizations (Theofanopoulou et al., 2017; Winslow et al., 2000). These data together with our findings suggest that SRPX2 protein expression in the hypothalamus, like in the language cortex, may also play a role in ultrasonic or verbal communication.

Most of the SRPX2-ir neurons were located in the Pa, which has three functional compartments. These include the neurosecretory magnocellular neurons projecting to the posterior pituitary, the neuroendocrine parvocellular neurons projecting to the median eminence, and the pre-autonomic parvocellular neurons projecting to the nucleus tractus solitarius, rostral ventrolateral medulla, and spinal cord (Ferguson et al., 2008; Loewen et al., 2017; Swanson & Sawchenko, 1983). This explains the observed topographic organization of SRPX2-ir projections to the hypophysis and brainstem.

The hypothalamus-pituitary axis regulates the fundamental endocrine and autonomic functions necessary for survival in both rodents and humans. Hypothalamic injury may lead to chronic pituitary dysfunction (Tanriverdi et al., 2015). For instance, vasopressin-expressing neurons regulate the water balance in the body, and their dysregulation due to traumatic brain injury (TBI) causes diabetes insipidus (Capatina, Paluzzi, Mitchell, & Karavitaki, 2015). Taken together, in addition to language development, SRPX2 protein mediated mechanisms can present a novel target to modulate neuroendocrine and autonomic functions of the hypothalamo-pituitary and hypothalamo-brainstem axis in normal and diseased brain.

References

Armstrong, J., Taylor, G., Thomas, H., Boddy, A., Redfern, C., & Veal, G. (2007). Molecular targeting of retinoic acid metabolism in neuroblastoma: the role of the CYP26 inhibitor R116010 in vitro and in vivo. *British Journal of Cancer*, *96*, 1675–1683.

Capatina, C., Paluzzi, A., Mitchell, R., & Karavitaki, N. (2015). Diabetes Insipidus after Traumatic Brain Injury. *Journal of Clinical Medicine*, *4*(7), 1448–1462.

Ferguson, A. V, Latchford, K. J., & Samson, W. K. (2008). The paraventricular nucleus of the hypothalamus – a potential target for integrative treatment of autonomic dysfunction. *Expert Opinion on Therapeutic Targets*, *12*(6), 717–727.

Huusko, N., Römer, C., Ndode-Ekane, X. E., Lukasiuk, K., & Pitkänen, A. (2015). Loss of hippocampal interneurons and epileptogenesis: a comparison of two animal models of acquired epilepsy. *Brain Structure & Function*, *220*(1), 153–91.

Kurosawa, H., Goi, K., Inukai, T., Inaba, T., Chang, K. S., Shinjyo, T., … Look, a T. (1999). Two candidate downstream target genes for E2A-HLF. *Blood*, *93*(1), 321–332.

Lesca, G., Rudolf, G., Bruneau, N., Lozovaya, N., Labalme, A., Boutry-Kryza, N., … Szepetowski, P. (2013). GRIN2A mutations in acquired epileptic aphasia and related childhood focal epilepsies and encephalopathies with speech and language dysfunction. *Nature Genetics*, *45*(9), 1061–6.

Lewis, D. A., Campbell, M. J., & Morrison, J. H. (1986). An immunohistochemical characterization of somatostatin-28 and somatostatin-281-12 in monkey prefrontal cortex. *The Journal of Comparative Neurology*, *248*(1), 1–18.

Lin, X., Chang, W., Wang, Y., Tian, M., & Yu, Z. (2017). SRPX2, an independent prognostic marker, promotes cell migration and invasion in hepatocellular carcinoma. *Biomedicine & Pharmacotherapy*, *93*, 398–405.

Liu, K., Fan, J., & Wu, J. (2017). Sushi repeat-containing protein X-linked 2 promotes angiogenesis through the urokinase-type plasminogen activator receptor dependent integrin αvβ3/focal adhesion kinase pathways. *Drug Discoveries & Therapeutics*, *11*(4), 212–217.

Liu, K. L., Wu, J., Zhou, Y., & Fan, J. H. (2015). Increased Sushi repeat-containing protein X-linked 2 is associated with progression of colorectal cancer. *Medical Oncology (Northwood, London, England)*, *32*(4), 99.

Loewen, S. P., Paterson, A. R., Loh, S. Y., Rogers, M. F., Hindmarch, C. C. T., Murphy, D., & Ferguson, A. V. (2017). Sex-specific differences in cardiovascular and metabolic hormones with integrated signalling in the paraventricular nucleus of the hypothalamus. *Experimental Physiology*, *0*(11), 1–7.

MacDermot, K. D., Bonora, E., Sykes, N., Coupe, A.-M., Lai, C. S. L., Vernes, S. C., … Fisher, S. E. (2005). Identification of FOXP2 Truncation as a Novel Cause of Developmental Speech and Language Deficits. *The American Journal of Human Genetics*, *76*(6), 1074–1080.

Ndode-Ekane, X. E., Hayward, N., Gröhn, O., & Pitkänen, A. (2010). Vascular changes in epilepsy: functional consequences and association with network plasticity in pilocarpine-induced experimental epilepsy. *Neuroscience*, *166*(1), 312–332.

Øster, B., Linnet, L., Christensen, L. L., Thorsen, K., Ongen, H., Dermitzakis, E. T., … Andersen, C. L. (2013). Non-CpG island promoter hypomethylation and miR-149 regulate the expression of SRPX2 in colorectal cancer. *International Journal of Cancer. Journal International Du Cancer*, *132*(10), 2303–15.

Pfundmair, M., Lamprecht, F., von Wedemeyer, F. M., & Frey, D. (2016). Your word is my command: Oxytocin facilitates the understanding of appeal in verbal communication. *Psychoneuroendocrinology*, *73*, 63–66.

Roll, P., Rudolf, G., Pereira, S., Royer, B., Scheffer, I. E., Massacrier, A., … Szepetowski, P. (2006). SRPX2 mutations in disorders of language cortex and cognition. *Human Molecular Genetics*, *15*(7), 1195–1207.

Roll, P., Vernes, S. C., Bruneau, N., Cillario, J., Ponsole-Lenfant, M., Massacrier, A., … Szepetowski, P. (2010). Molecular networks implicated in speech-related disorders: FOXP2 regulates the SRPX2/uPAR complex. *Human Molecular Genetics*, *19*(24), 4848–60.

Royer-Zemmour, B., Ponsole-Lenfant, M., Gara, H., Roll, P., Lévêque, C., Massacrier, A., … Szepetowski, P. (2008). Epileptic and developmental disorders of the speech cortex: ligand/receptor interaction of wild-type and mutant SRPX2 with the plasminogen activator receptor uPAR. *Human Molecular Genetics*, *17*(23), 3617–30.

Salmi, M., Bruneau, N., Cillario, J., Lozovaya, N., Massacrier, A., Buhler, E., … Szepetowski, P. (2013). Tubacin prevents neuronal migration defects and epileptic activity caused by rat Srpx2

silencing in utero. *Brain : A Journal of Neurology*, *136*(Pt 8), 2457–73.

Schmittgen, T. D., & Livak, K. J. (2008). Analyzing real-time PCR data by the comparative CT method. *Nature Protocols*, *3*(6), 1101–1108.

Sia, G. M., Clem, R. L., & Huganir, R. L. (2013). The human language-associated gene SRPX2 regulates synapse formation and vocalization in mice. *Science (New York, N.Y.)*, *342*(6161), 987–991.

Swanson, L. W., & Sawchenko, P. E. (1983). Hypothalamic Integration: Organization of the Paraventricular and Supraoptic Nuclei. *Annual Review of Neuroscience*, *6*(1), 269–324.

Tanaka, K., Arao, T., Maegawa, M., Matsumoto, K., Kaneda, H., Kudo, K., … Nishio, K. (2009). SRPX2 is overexpressed in gastric cancer and promotes cellular migration and adhesion. *International Journal of Cancer*, *124*(5), 1072–1080.

Tang, H., Zhao, J., Zhang, L., Zhao, J., Zhuang, Y., & Liang, P. (2016a). SRPX2 Enhances the Epithelial-Mesenchymal Transition and Temozolomide Resistance in Glioblastoma Cells. *Cellular and Molecular Neurobiology*, *36*(7), 1067–76.

Tang, H., Zhao, J., Zhang, L., Zhao, J., Zhuang, Y., & Liang, P. (2016b). SRPX2 Enhances the Epithelial???Mesenchymal Transition and Temozolomide Resistance in Glioblastoma Cells. *Cellular and Molecular Neurobiology*, *36*(7), 1067–1076.

Tanriverdi, F., Schneider, H. J., Aimaretti, G., Masel, B. E., Casanueva, F. F., & Kelestimur, F. (2015). Pituitary dysfunction after traumatic brain injury: a clinical and pathophysiological approach. *Endocrine Reviews*, *36*(3), 305–42.

Theofanopoulou, C., Boeckx, C., & Jarvis, E. D. (2017). A hypothesis on a role of oxytocin in the social mechanisms of speech and vocal learning. *Proceedings of the Royal Society B: Biological Sciences*, *284*(1861), 20170988.

Uhlen, M., Bandrowski, A., Carr, S., Edwards, A., Ellenberg, J., Lundberg, E., … Yamamoto, T. (2016). A proposal for validation of antibodies. *Nature Methods*, *13*(10), 823–827.

van Vliet, E. A., Puhakka, N., Mills, J. D., Srivastava, P. K., Johnson, M. R., Roncon, P., … Pitkänen, A. (2017). Standardization procedure for plasma biomarker analysis in rat models of epileptogenesis: Focus on circulating microRNAs. *Epilepsia*, 1–12.

West, M. J., Slomianka, L., & Gundersen, H. J. (1991). Unbiased stereological estimation of the total number of neurons in thesubdivisions of the rat hippocampus using the optical fractionator. *The Anatomical Record*, *231*(4), 482–97.

Winslow, J. T., Hearn, E. F., Ferguson, J., Young, L. J., Matzuk, M. M., & Insel, T. R. (2000). Infant Vocalization, Adult Aggression, and Fear Behavior of an Oxytocin Null Mutant Mouse. *Hormones and Behavior*, *37*(2), 145–155.

Yamada, T., Oshima, T., Yoshihara, K., Sato, T., Nozaki, A., Shiozawa, M., … Masuda, M. (2014). Impact of overexpression of Sushi repeat-containing protein X-linked 2 gene on outcomes of gastric cancer. *Journal of Surgical Oncology*, *109*(8), 836–40.

Ye, Z., Stolk, A., Toni, I., & Hagoort, P. (2016). Oxytocin Modulates Semantic Integration in Speech Comprehension. *Journal of Cognitive Neuroscience*, *29*(2), 1–10.

Zhang, H. F., Dai, Y. C., Wu, J., Jia, M. X., Zhang, J. S., Shou, X. J., … Han, J. S. (2016). Plasma Oxytocin and Arginine-Vasopressin Levels in Children with Autism Spectrum Disorder in China: Associations with Symptoms. *Neuroscience Bulletin*, *32*(5), 423–432.

Figure legends

Figure 1: Polyclonal rabbit anti-SRPX2 (ab91584) specifically detected SRPX2 protein in SH-SY5Y neuroblastoma cells. SRPX2 positive immunostaining (green, anti-SRPX2 ab91584) in **(a)** mouse N2a neuroblastoma cells, **(b)** human n2012 cells and **(c)** human SH-SY5Y cells with DAPI counterstaining (blue). **(d)** SH-SY5Y cells transfected with 30 and 50 nM *SRPX2* siRNA showed a 54% and 87% decrease, respectively, in *SRPX2* mRNA levels as determined by qPCR. The knockdown resulted in decreased SRPX2 protein levels in SH-SY5Y cells in **(e)** Western blot (SRPX2 53 kDa and β-actin 43 kDa) and **(f-h)** immunofluorescence labeling **[(f)** untreated, **(g)** negative control siRNA, **(h)** *SRPX2* siRNA (50 nM)**]**. **(i)** FAM-labeled negative control siRNA (green) was transported across the cell membranes of SRPX2 labeled (red) SH-SY5Y cells by the Lipofectamine® 2000, demonstrating good transfection efficiency. The photomicrograph was taken 24 h after transfection. **(j)** The MTT assay showed a trend towards a slight decrease (~20%, $p>0.05$ using Kruskal-Wallis test) in cell viability in SH-SY5Y cells after transfection as compared with untreated cells. Scale bar equals (a-c) 20 µm (f-i) 50 µm.

Figure 2: SRPX2 is expressed in hypothalamic neurons of the rat and human brain. *In situ* hybridization confirmed the presence of *SRPX2* mRNA in **(a)** the rat and **(b)** the human hypothalamus (paraventricular nucleus shown). Immunohistochemical labeling of SRPX2 protein by anti-SRPX2 antibody was also detected in the same hypothalamic nuclei in **(c)** rat and **(d)** human. **(e)** SRPX2 protein (red, anti-SRPX2 ab91584) colocalized with *SRPX2* mRNA (purple, arrows) as seen by immunohistochemistry and *in situ* hybridization, respectively. **(f)** SRPX2 positive immunostaining was reproduced in the paraventricular nucleus of the hypothalamus of the rat brain (brown, arrows) using mouse monoclonal anti-SRPX2 antibody (1:1000, 66266-1, Proteintech). **(g)** SRPX2 mRNA expression was markedly less in the human cortex compared with the hypothalamus using RT-qPCR (Data expressed as mean ± SEM). Double labelling of SRPX2-ir **(h, k)** neurons with astrocyte marker, GFAP **(i)** and microglia marker, OX-42 **(l)** showed no colocalization **(j, m)**. Scale bars equal (a-e) 50 µm, (f) 100 µm (h-m) 20 µm.

Figure 3: SRPX2 expression in the hypothalamus is highly conserved in the rodent, non-human primate, and human brain. SRPX2 protein in the rat hypothalamus: **(a)** bilateral distribution of SRPX2-ir neurons in the paraventricular (a_1, Pa), periventricular (a_1, Pe) and supraoptic nuclei (a_2, SO). **(b)** A darkfield photomicrograph showing dense SRPX2 immunoreactive projections (white arrow) in the hypothalamus, which turned caudally towards the hypophysis. **(c)** A higher-magnification photomicrograph of a paraffin-embedded thionin-counterstained section, showing SRPX2 positive neurons in the rat Pa. Note the granular appearance of the positive cytosolic staining. SRPX2-ir neurons in the Pa, Pe and SO nuclei in the **(d)** mouse **(e)** monkey, and **(f)** human hypothalamus. The insets in the upper left corner show the immunopositive neurons in each species in the area indicated with dashed boxes. Scale bars: (a, d-f) 500 µm, (b) 200 µm, (c) 10 µm, (a_1-a_2, b_1-f_1) 50 µm.

Figure 4: SRPX2-ir axonal staining in the median eminence and the brainstem. SRPX2-ir fibers in the internal zone of the median eminence of the rat brain under **(a)** bright-field and **(b)** dark-field illuminations. SRPX2-positive terminals in the nucleus of the solitary tract (NTS) in rat under **(c)** bright-field and **(d)** dark-field illuminations. The insets show higher-magnification photomicrographs of varicosities and intervaricose segments of the SRPX2-ir terminals under (c_1) bright-field and (d_1) dark-field illuminations. Scale bars: (a-b) 50 µm (c-d) 20 µm (c_1-d_1) 10 µm.

Figure 5: SRPX2 protein distribution in the hypothalamo-hypophyseal axis. Colocalization of SRPX2-ir (rabbit polyclonal anti-SRPX2) **(a)** with oxytocin-ir **(b)** neurons (**c** merged), and SRPX2-ir (mouse monoclonal anti-SRPX2) **(d)** with vasopressin-ir **(e)** neurons (**f** merged) in the Pa and SO (a_1-f_1) nuclei of rat hypothalamus. **(c_2)** Insert showing a higher-magnification photomicrograph of SRPX2-ir granules in the cytoplasm of oxytocin-ir neuron of Pa. Photomicrographs showing SRPX2 immunoreactivity in rat neurohypophysis under **(g)** bright-field and **(h)** dark-field illumination and human neurohypophysis under **(j)** bright-field and **(k)** dark-field illumination with and without (j_1, k_1) thionin counterstaining. SRPX2-ir secretory cells of **(i)** rat and **(l)** human adenohypophysis counterstained with thionin. (i_1, l_1) Higher-magnification photomicrograph showing the cytoplasmic staining. **(m)** Western blot showing SRPX2-ir bands in rat plasma, human plasma, and human CSF. Scale bars: (a-f, a_1-f_1) 100 µm, (g-l, j_1- k_1) 40 µm, (i_1) 15 µm, (c_2, l_1) 5 µm.

John Wiley & Sons

Figure 6: A schematic illustration showing the distribution of the SRPX2-ir neurons (in blue) in the hypothalamus and the fibers (in red) in the hypothalamus, dorsal and ventral raphe nuclei, locus coeruleus, and the nucleus of solitary tract of the rat brain (adapted from The Paxinos Rat Brain Atlas).

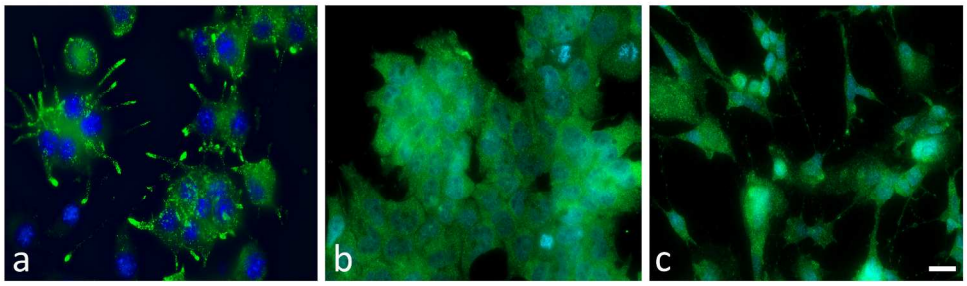

SRPX2 siRNA (nM)	Fold change	Knock down (%)
30 nM	-2.19	54.3
50 nM	-8.22	87.8

d

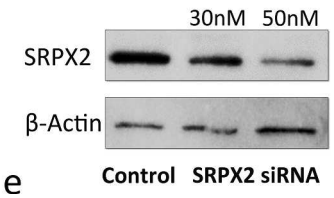

e

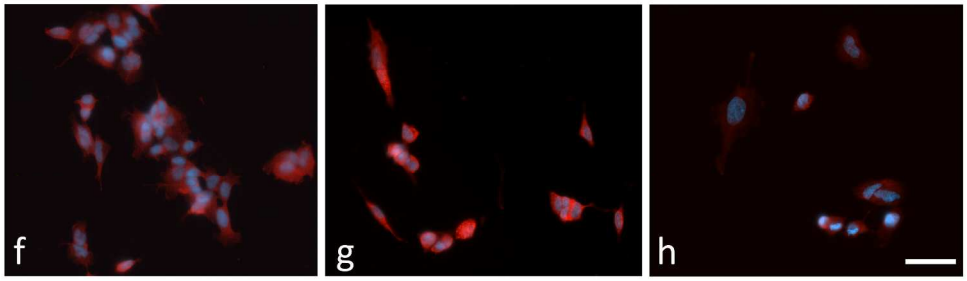

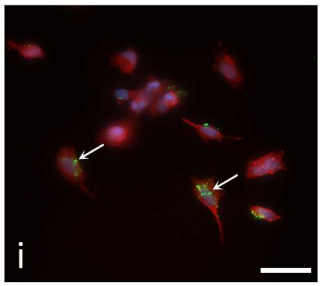

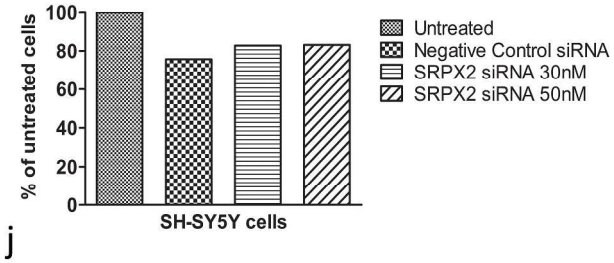

j

Figure 1: Polyclonal rabbit anti-SRPX2 (ab91584) specifically detected SRPX2 protein in SH-SY5Y neuroblastoma cells. SRPX2 positive immunostaining (green, anti-SRPX2 ab91584) in (a) mouse N2a neuroblastoma cells, (b) human n2012 cells and (c) human SH-SY5Y cells with DAPI counterstaining (blue). (d) SH-SY5Y cells transfected with 30 and 50 nM SRPX2 siRNA showed a 54% and 87% decrease, respectively, in SRPX2 mRNA levels as determined by qPCR. The knockdown resulted in decreased SRPX2 protein levels in SH-SY5Y cells in (e) Western blot (SRPX2 53 kDa and β-actin 43 kDa) and (f-h) immunofluorescence labeling [(f) untreated, (g) negative control siRNA, (h) SRPX2 siRNA (50 nM)]. (i) FAM-labeled negative control siRNA (green) was transported across the cell membranes of SRPX2 labeled (red) SH-SY5Y cells by the Lipofectamine® 2000, demonstrating good transfection efficiency. The photomicrograph was taken 24 h after transfection. (j) The MTT assay showed a trend towards a slight decrease (~20%, $p>0.05$ using Kruskal-Wallis test) in cell viability in SH-SY5Y cells after transfection as compared with untreated cells. Scale bar equals (a-c) 20 μm (f-i) 50 μm.

350x408mm (300 x 300 DPI)

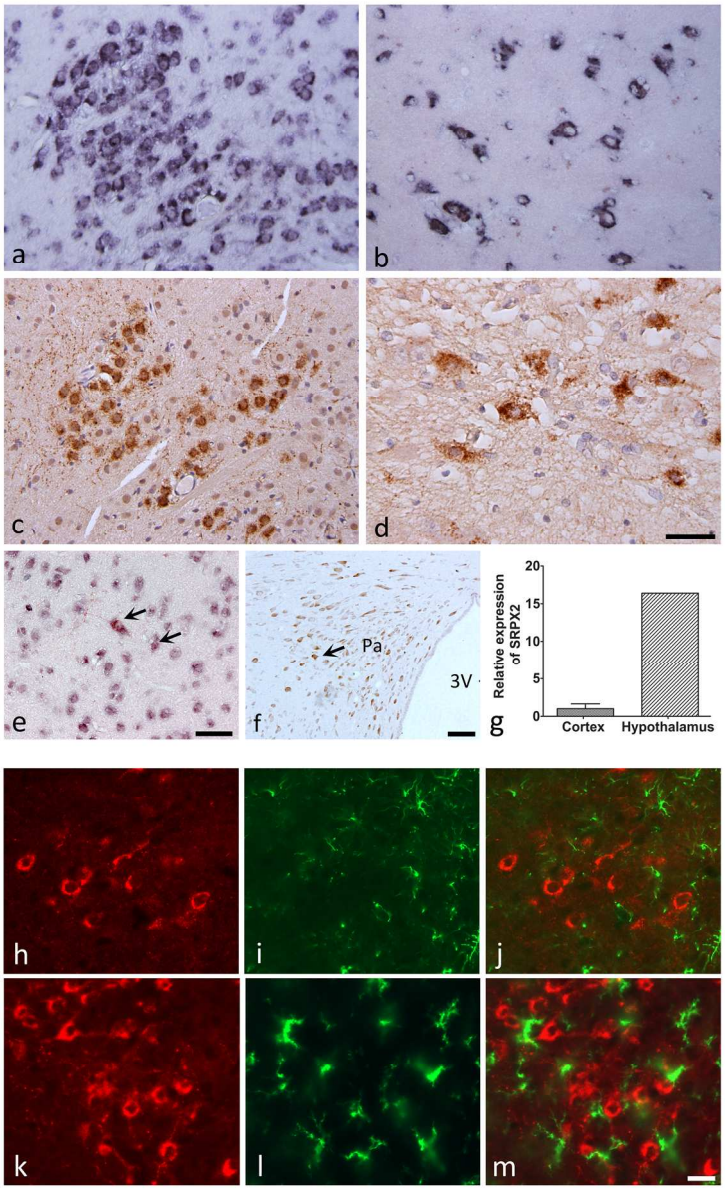

Figure 2: SRPX2 is expressed in hypothalamic neurons of the rat and human brain. In situ hybridization confirmed the presence of SRPX2 mRNA in (a) the rat and (b) the human hypothalamus (paraventricular nucleus shown). Immunohistochemical labeling of SRPX2 protein by anti-SRPX2 antibody was also detected in the same hypothalamic nuclei in (c) rat and (d) human. (e) SRPX2 protein (red, anti-SRPX2 ab91584) colocalized with SRPX2 mRNA (purple, arrows) as seen by immunohistochemistry and in situ hybridization, respectively. (f) SRPX2 positive immunostaining was reproduced in the paraventricular nucleus of the hypothalamus of the rat brain (brown, arrows) using mouse monoclonal anti-SRPX2 antibody (1:1000, 66266-1, Proteintech). (g) SRPX2 mRNA expression was markedly less in the human cortex compared with the hypothalamus using RT-qPCR (Data expressed as mean ± SEM). Double labelling of SRPX2-ir (h, k) neurons with astrocyte marker, GFAP (i) and microglia marker, OX-42 (l) showed no colocalization (j, m). Scale bars equal (a-e) 50 µm, (f) 100 µm (h-m) 20 µm.

160x264mm (300 x 300 DPI)

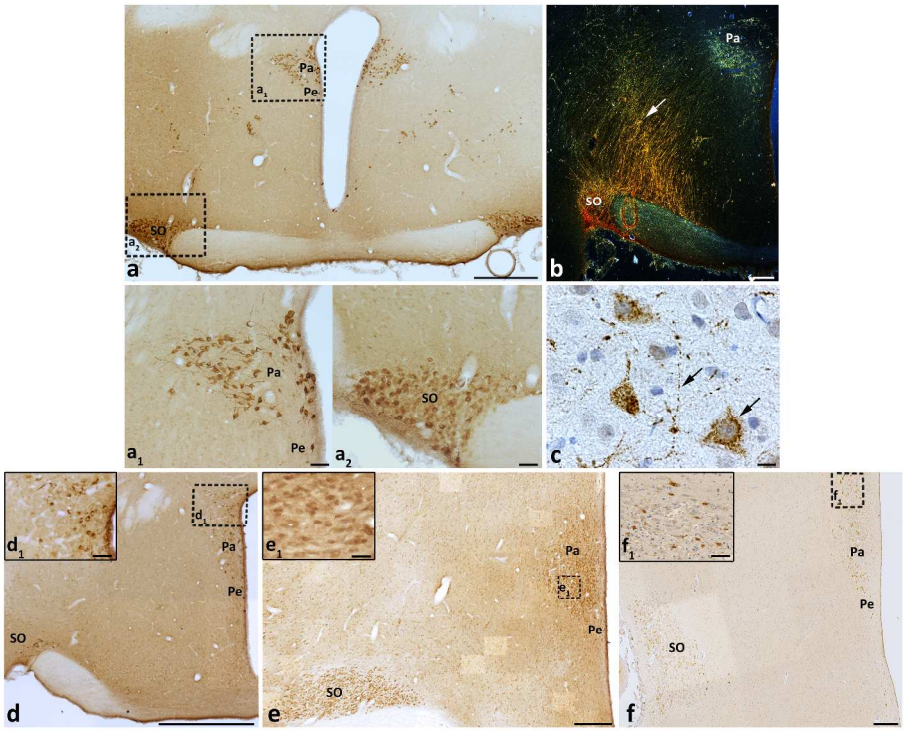

Figure 3: SRPX2 expression in the hypothalamus is highly conserved in the rodent, non-human primate, and human brain. SRPX2 protein in the rat hypothalamus: (a) bilateral distribution of SRPX2-ir neurons in the paraventricular (a1, Pa), periventricular (a1, Pe) and supraoptic nuclei (a2, SO). (b) A darkfield photomicrograph showing dense SRPX2 immunoreactive projections (white arrow) in the hypothalamus, which turned caudally towards the hypophysis. (c) A higher-magnification photomicrograph of a paraffin-embedded thionin-counterstained section, showing SRPX2 positive neurons in the rat Pa. Note the granular appearance of the positive cytosolic staining. SRPX2-ir neurons in the Pa, Pe and SO nuclei in the (d) mouse (e) monkey, and (f) human hypothalamus. The insets in the upper left corner show the immunopositive neurons in each species in the area indicated with dashed boxes. Scale bars: (a, d-f) 500 μm, (b) 200 μm, (c) 10 μm, (a1-a2, b1-f1) 50 μm.

500x374mm (300 x 300 DPI)

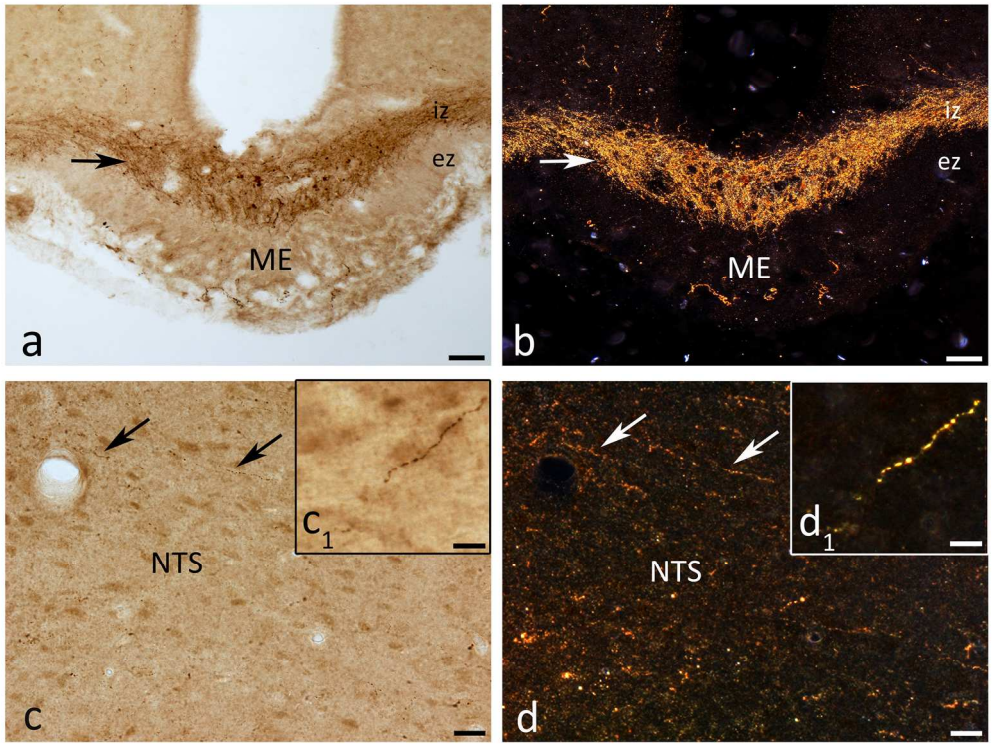

Figure 4: SRPX2-ir axonal staining in the median eminence and the brainstem. SRPX2-ir fibers in the internal zone of the median eminence of the rat brain under (a) bright-field and (b) dark-field illuminations. SRPX2-positive terminals in the nucleus of the solitary tract (NTS) in rat under (c) bright-field and (d) dark-field illuminations. The insets show higher-magnification photomicrographs of varicosities and intervaricose segments of the SRPX2-ir terminals under (c1) bright-field and (d1) dark-field illuminations.

240x182mm (300 x 300 DPI)

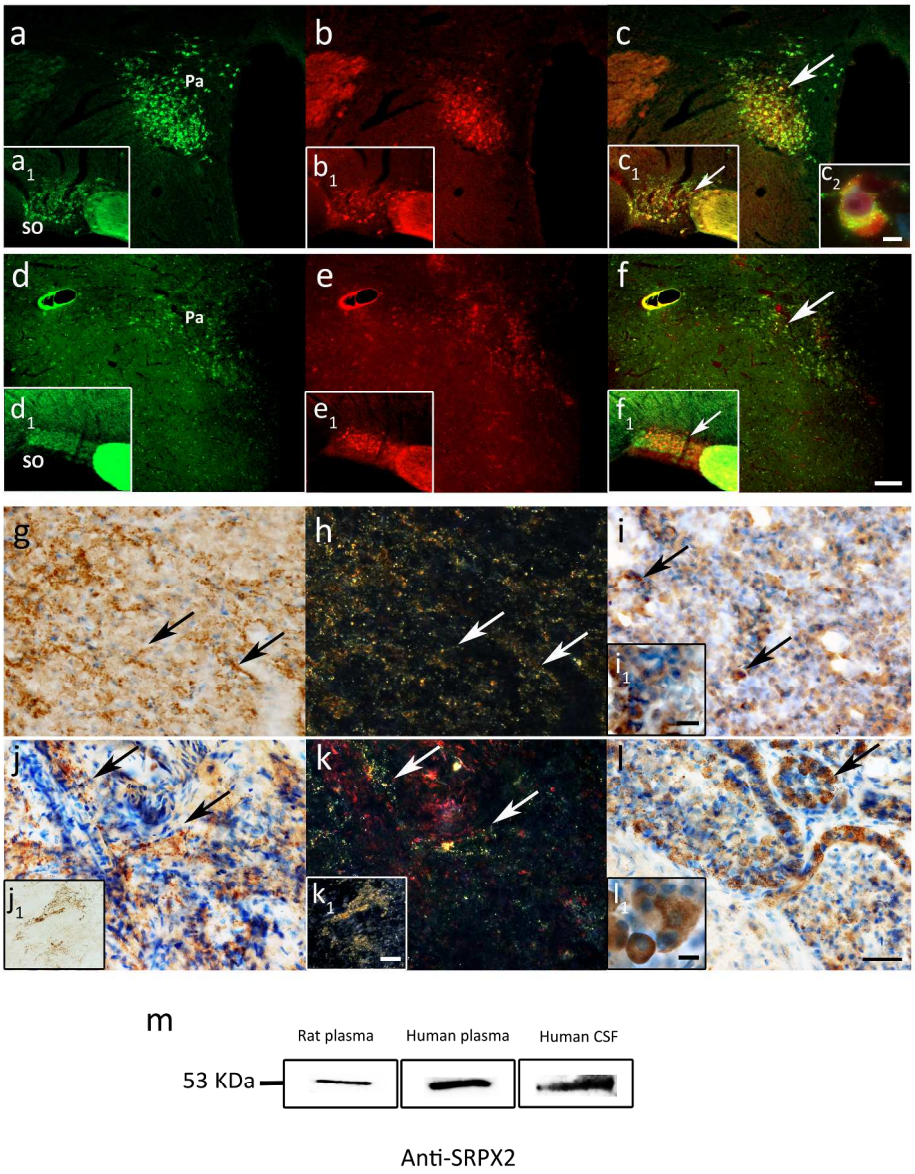

Figure 5: SRPX2 protein distribution in the hypothalamo-hypophyseal axis. Colocalization of SRPX2-ir (rabbit polyclonal anti-SRPX2) (a) with oxytocin-ir (b) neurons (c merged), and SRPX2-ir (mouse monoclonal anti-SRPX2) (d) with vasopressin-ir (e) neurons (f merged) in the Pa and SO (a1-f1) nuclei of rat hypothalamus. (c2) Insert showing a higher-magnification photomicrograph of SRPX2-ir granules in the cytoplasm of oxytocin-ir neuron of Pa. Photomicrographs showing SRPX2 immunoreactivity in rat neurohypophysis under (g) bright-field and (h) dark-field illumination and human neurohypophysis under (j) bright-field and (k) dark-field illumination with and without (j1, k1) thionin counterstaining. SRPX2-ir secretory cells of (i) rat and (l) human adenohypophysis counterstained with thionin. (i1, l1) Higher-magnification photomicrograph showing the cytoplasmic staining. (m) Western blot showing SRPX2-ir bands in rat plasma, human plasma, and human CSF. Scale bars: (a-f, a1-f1) 100 µm, (g-l, j1- k1) 40 µm, (i1) 15 µm, (c2, l1) 5 µm.

399x474mm (300 x 300 DPI)

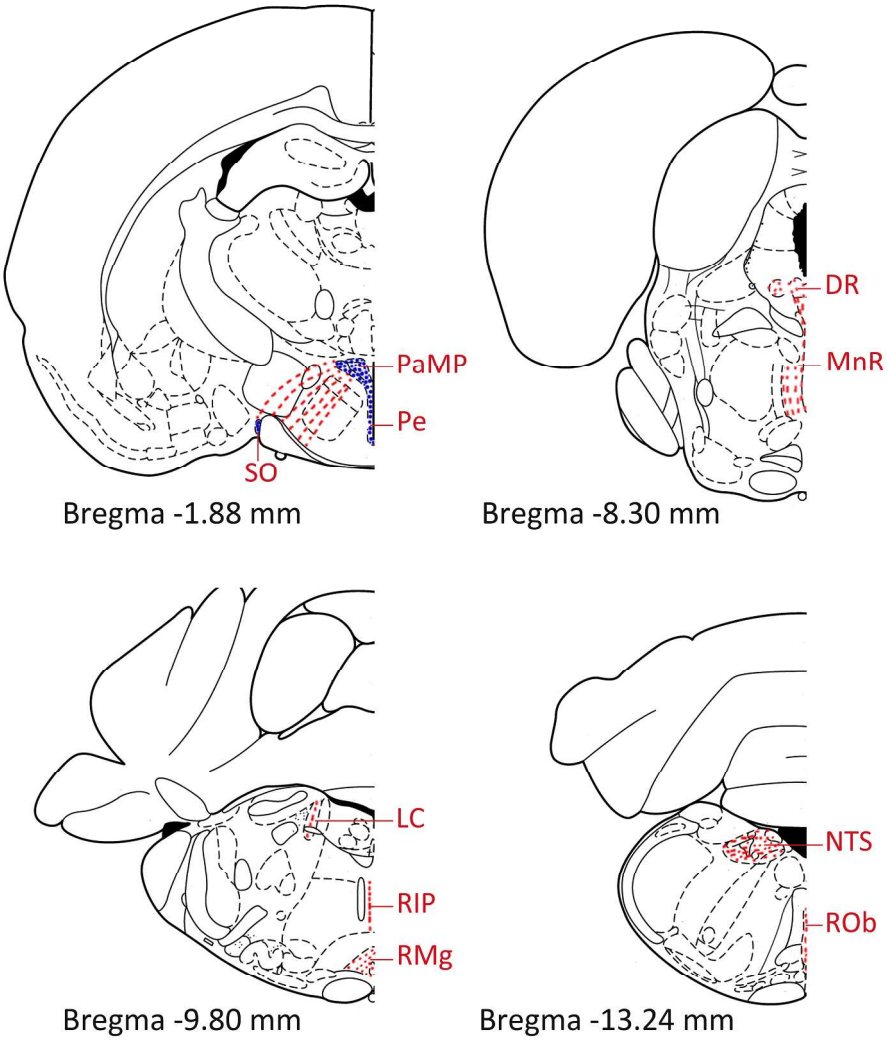

Figure 6: A schematic illustration showing the distribution of the SRPX2-ir neurons (in blue) in the hypothalamus and the fibers (in red) in the hypothalamus, dorsal and ventral raphe nuclei, locus coeruleus, and the nucleus of solitary tract of the rat brain (adapted from The Paxinos Rat Brain Atlas).

350x389mm (300 x 300 DPI)

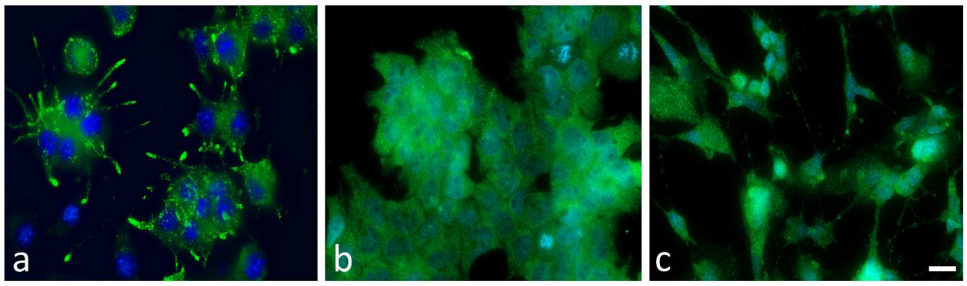

d

SRPX2 siRNA (nM)	Fold change	Knock down (%)
30 nM	-2.19	54.3
50 nM	-8.22	87.8

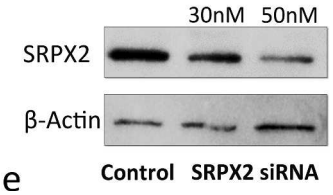

e

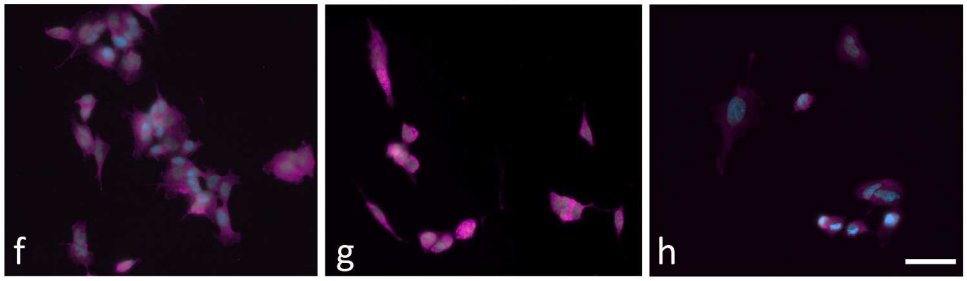

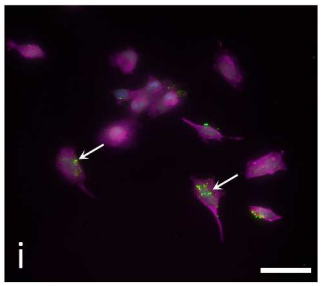

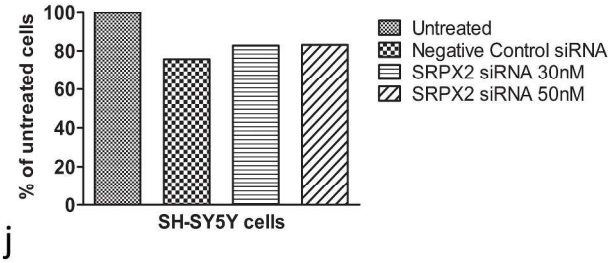

j

650x758mm (150 x 150 DPI)

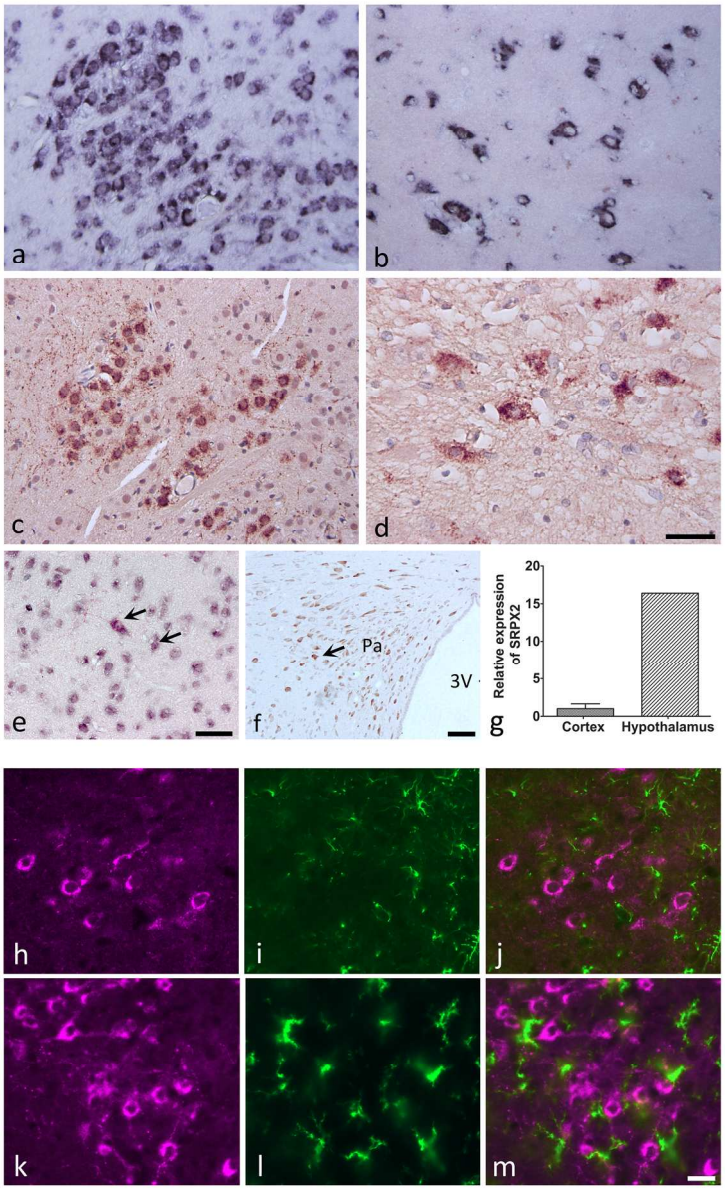

160x264mm (300 x 300 DPI)

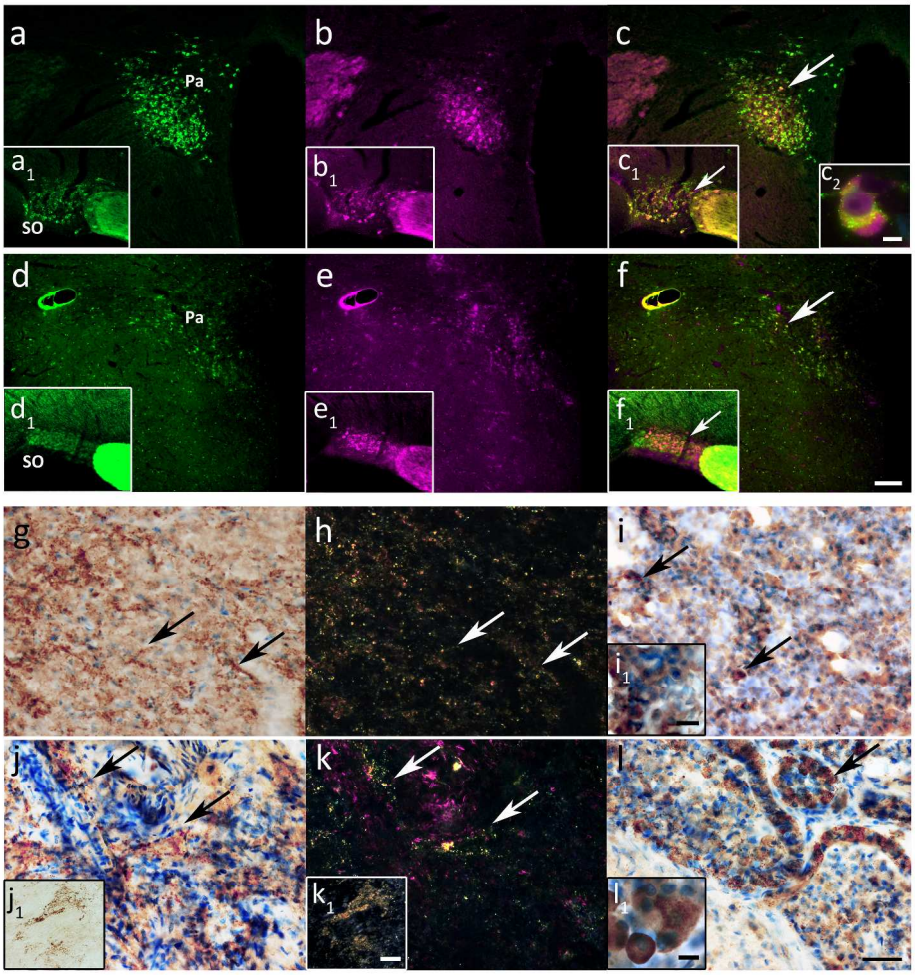

Anti-SRPX2

299x355mm (300 x 300 DPI)

Graphical Abstract Text

We identified a unique phylogenetically conserved distribution of SRPX2 protein in the hypothalamic paraventricular, periventricular, and supraoptic nuclei, and demonstrated that the axons of these SRPX2-immunoreactive neurons project to the hypophysis and brainstem. We also identified its colocalization with oxytocin or vasopressin, and detected SRPX2 protein in plasma and CSF.

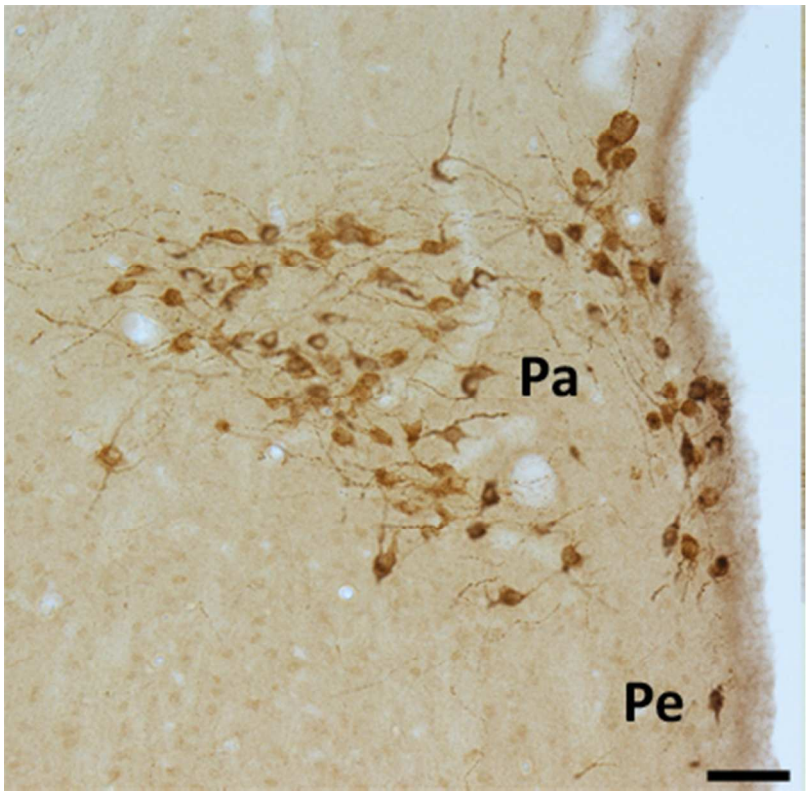

141x138mm (72 x 72 DPI)